Iranian Journal of Livestock Science, 2024, VOL. 1, NO. 1: 33-40

Iranian Journal of Livestock Science

journal homepage: **www.ijls.yu.ac.ir**

A frameshift mutation (c.1021delC) in GCGR in *Gallus varius* may interpret its higher blood glucose level in comparison to *G. gallus*

Fatemeh Dashti[1*], Karim Mahnam[2, 3], Mostafa Shakhsi-Niaei[1, 3]

[1]*Department of Genetics, Faculty of Basic Sciences, Shahrekord University, Shahrekord, Iran*
[2]*Department of Biology, Faculty of Basic Sciences, Shahrekord University, Shahrekord, Iran*
[3]*Research Institute of Biotechnology, Shahrekord University, Shahrekord, Iran*

Article Info

© 2024 the authors. Published by Yasouj University, Yasouj, Iran. This is an open access article under the terms of the Creative Commons Attribution 4.0 International License.

Iranian Journal of Livestock Science, 2024, VOL. 1, No. 1: 33-40
https://doi.org/10.61186/IJLS.1.1.33

Article History
Received: April 7nd 2024
Revised: May 22th 2024
Accepted: June 2th 2024
Published: June 9th 2024

ABSTRACT

Blood glucose level is an important physiological factor that is controlled by hormones, hormone receptors, and certain regulatory proteins. Studies of various organisms have shown that the control and regulation of glucose is very different amongst organisms. The present study aimed to reconstruct the genes in *Gallus varius (G. varius)* and then to investigate possible genetic variations in genes involved in glucose homeostasis pathway between *Gallus gallus (G. gallus)* and *G. varius*. To this end, the *GIPR, GCGR, GLP-2R, GLP-1R, and GCG* genes in the Gallus family were identified as genes involved in blood glucose homeostasis from KEGG database. The nucleotide sequences of these genes from *G. gallus* were obtained in FASTA format from the NCBI database and blasted with tblastn tools with SRAs related to *G. varius*. Then, the nucleotide and amino acid sequences of these genes for *G. varius* were predicted and their polymorphisms with corresponding genes in *G. gallus* were identified. The results indicated different variations in considered genes consisting a single nucleotide deletion in the *G. varius* glucagon receptor which leads to a frameshift and premature stop codon in *GCGR* gene. This mutation deletes last two transmembrane domains of this receptor. The results of molecular dynamics simulations also confirmed the dramatic changes in the structure of the glucagon receptor gene. To sum up, it is suggested that the blood glucose variation can be investigated between these two species during different physiological situations such as fasting or feeding in birds to elucidate the effect of this mutation, in this important blood glucose homeostasis gene.

Keywords: Glucose homeostasis, *G. gallus*, *G. varius*, frameshift mutation, GCGR gene

INTRODUCTION

The concentration of glucose in the bloodstream is regulated by a complex interplay of hormones, their receptors, and distinct regulatory proteins (Idowu and Heading, 2018). Research examining various species indicates that the mechanisms governing glucose balance can vary greatly among different life forms (Braun and Sweazea, 2008). Mammals typically maintain blood glucose levels around 7 mM, and while fish and amphibians typically exhibit lower blood glucose levels compared to mammals (Polakof *et al.*, 2012), its level is generally double in birds (Zhang *et al.*, 2018). A recent study has shown that body mass is inversely related to blood glucose concentrations, and birds with lower body mass have higher blood glucose concentrations (Norris and Carr, 2021). On the other hand, another study has identified species-specific differences in blood glucose level even among birds (Braun and Sweazea, 2008). Interestingly, it is mentioned

***Corresponding author**
Postal Address: *Department of Genetics, Faculty of Basic Sciences, Shahrekord University, Shahrekord, Iran. Postal code: 8818634141*
E-mail: Shakhsi-niaei.m@sku.ac.ir

[Downloaded from ijls.yu.ac.ir on 2025-10-16]

[DOI: 10.61186/ijls.1.1.33]

that blood glucose level in *G. varius* (19.95 mM) is about 1.5 times more than *G. gallus* (13.37 mM), which both are two species from the same genus (Teare, 2013). However, the genetic mechanism behind blood glucose level has not yet been extensively investigated in vertebrates (Mendowski *et al.*, 2020).

In this study, we investigated the genes involved in blood glucose homeostasis to elucidate the genetic variations that contribute to different blood glucose levels. This was done considering the two phylogenetically close species with significantly different blood glucose levels, *G. gallus* (red jungle fowl) and *G. varius* (green jungle fowl). The genome of *G. varius* is not available in genome databases, but un-mapped sequences are accessible in the Sequence Read Archive (**SRA**) database. Consequently, this research aims to reconstruct the target genes of *G. varius* from this database. It will then investigate the potential genetic differences in the genes of the glucose homeostasis pathway between *G. gallus* and *G. varius*.

MATERIALS AND METHODS

In this research, the KEGG database was utilized to identify genes involved in the glucose homeostasis of *G. gallus*. By text mining, we could locate the *GIPR*, *GCGR*, *GLP-2R*, *GLP-1R*, and *GCG* genes involved in blood glucose homeostasis. From the NCBI database, the nucleotide sequences of the *GIPR* (XM_025144504.1), *GCGR* (NM_001101035.1), *GLP-2R* (NM_001163248.1), *GLP-1R* (NM_001135551.1), and *GCG* (NM_001190165.4) genes were retrieved in FASTA format for *G. gallus*, along with SRA data related to *G. varius*. Briefly, the complete sequence of the mRNA for each gene was blasted against the related SRA accession numbers, when the SRA database was selected as the database (from the Database drop-down list) using blastn (https://blast.ncbi.nlm.nih.gov/Blast.cgi?PROGRAM=blastn&PAGE_TYPE=BlastSearch&BLAST_SPEC=&LINK_LOC=blasttab&LAST_PAGE=blastn). These sequences were then compared using tblastn (https://blast.ncbi.nlm.nih.gov/Blast.cgi?PROGRAM=tblastn&PAGE_TYPE=BlastSearch) to identify polymorphisms between two species. Nucleotide and amino acid sequences of selected genes in *G. varius* were predicted from *G. gallus* as template, using various SRAs available on the NCBI site, taking into account the greatest overlap with the reference genes.

The online translation tool ExPASy Translate (https://web.expasy.org/translate/ https://web.expasy.org/translate/) was employed to translate the nucleotide sequences of *G. varius* genes, and the amino acid sequence was subsequently predicted.

The sequences were aligned to determine the degree of similarity between the amino acid sequences of *G. gallus* and *G. varius*, to identify conserved regions, and to assess the significance of mutations derived from the reconstruction of glucose homeostasis genes in *G. varius*, using the Clustal Omega server (https://www.ebi.ac.uk/jdispatcher/msa/clustalo).

To model the GCGR protein in two selected species previously available structures of GCGR from other organisms with most similarity to our GCGR sequences were required. For this purpose, the sequences of GCGR proteins from *G. gallus* and *G. varius* were inserted into the blastp server (https://blast.ncbi.nlm.nih.gov/Blast.cgi?PROGRAM=blastp&PAGE_TYPE=BlastSearch&BLAST_SPEC=&LINK_LOC=blasttab&LAST_PAGE=blastn). Therefore, we found the Chain R of a protein with the PDB code of 6wpw showed 67% identity E-value of zero, and 92% coverage with our blasted GCGR protein. The chain R of another protein with the PDB code of 6whc had 70% identity, E-value of zero, and 86% coverage as well. Also, the chain R of another protein with PDB code of 6lmk was recognized with 70% identity, E-value of zero, and 84% coverage. Modeller 10 software (Sali, 1993) was then used for multi-template modeling of the GCGR proteins of two species. Two thousand models were constructed for each variety, and the best models were selected based on DOPE (Discrete Optimized Protein Energy) scores. In the final step, the top models from the modeling phase were simulated using the GROMACS 2020 package (Abraham, 2015; Van der Spoel *et al.*,

[Downloaded from ijls.yu.ac.ir on 2025-10-16]

[DOI: 10.61186/ijls.1.1.33]

2005) under the Gromos force field (**G43A1**) (Berendsen *et al.*, 1995). The systems were neutralized by adding 6 Cl^- ions for *G. gallus* and 8 Cl^- for *G. varius*, along with approximately 30,000 SPC216 water model molecules. Fifty ns MD simulations for each GCGR model were performed in the NPT ensemble at 310 K with a time step of 1 fs. Simulations followed the methods described by Mahnam and Raisi (2017) and Mahnam *et al.* (2018).

The PROCHECK software was used for the G-factor analysis. The G-factor measures how "normal" or "unusual" dihedral angles are or the stereochemical properties of the model. The acceptable values of the overall G-factor in PROCHECK are between 0 and -0.5; values close to zero imply the best-quality models (Gundampati *et al.*, 2012).

Also, the Z-score was obtained from the Prosa site (https://prosa.services.came.sbg.ac.at/prosa.php). The Z-score indicates overall model quality and measures the deviation of the total energy of the structure considering an energy distribution derived from random conformations (Sippl, 1995).

RESULTS

The results of nucleotide sequence of *GIPR*, *GCGR*, *GLP-2R*, *GLP-1R*, and *GCG* genes in *G. gallus* and different SRXs related to *G. varius* are given in the appendix. The observed polymorphisms are listed in Table 1, which include synonymous, non-synonymous, and deletion mutations resulting in early termination codons. As it is known, a single nucleotide deletion occurred in the *GCGR* gene, which caused a frameshift mutation.

Table 1 The polymorphisms observed in the investigated genes between *G. gallus* and *G. varius*

Gene	Polymorphisms loci	Amino acid position	Amino acids in *G. gallus*	Amino acid in *G. varius*
GCG	c.120 T>C	40	Ser	Ser
	c.501 G>A	167	Ala	Ala
	c.510 C>T	170	Thr	Thr
GLP-1R	c.52 A>G	18	Arg	Gly
	c.952 C>T	318	Leu	Leu
	c.1104 T>C	368	Asp	Asp
GLP-2R	c.147 T>C	49	Asn	Asn
	c.267 T>C	89	Ser	Ser
	c.318 C>T	106	Asn	Asn
	c.346 A>G	116	Thr	Ala
	c.472 A>G	158	Ile	Val
	c.482 G>A	161	Cys	Tyr
	c.786 A>G	262	Thr	Thr
GCGR	c.144 T>C	48	Pro	Pro
	c.540 C>T	180	Ile	Ile
	c.681 C>T	227	Tyr	Tyr
	c.981 C>T	327	Leu	Leu
	c.1016 T>G	339	Phe	Cys
	c.1021 delC	341	Leu	Frame shift
GIPR	c.270 T>C	90	Cys	Cys
	c.426 C>T	142	Leu	Leu
	c.427 A>C	143	Ile	Leu
	c.531 C>G	177	Ala	Ala
	c.998 T>G	333	Leu	Trp
	c.1008 A>G	336	Ser	Ser
	c.1238 A>G	413	His	Arg
	c.1243 G>A	415	Ala	Thr
	c.1259 G>A	420	Arg	His
	c.1344 T>C	448	pro	Pro

[Downloaded from ijls.yu.ac.ir on 2025-10-16]

[DOI: 10.61186/ijls.1.1.33]

All the mutations that caused amino acid changes between the two species were investigated and according to the results obtained, the most severe mutation was further investigated.

The normalized DOPE energies for the best models of GCGR gene was 0.776 kcal/mol for *G. varius* and 0.926 kcal/mol for *G. gallus* The Ramachandran plot obtained from the Saves site (https://saves.mbi.ucla.edu/) showed that in the *G. varius* in the best model, 99.4%, of residues were in allowed regions, 0.6%, in generously allowed regions, and 0%, in disallowed regions. For *G. gallus,* the best model was 99.4% of residues were in allowed regions, 0.4% in generously allowed regions and 0.2% in disallowed regions (Figure 1). These results showed that the models are fine and proper for further analysis.

In addition, the total G-factor of PROCHECK software for the GCGR protein in *G. varius* and *G. gallus* was -0.01 and 0, respectively. Also, the Z-score obtained from the Prosa site was -4.86 and -3.85 of the GCGR protein for *G. gallus* and *G. varius,* respectively (Figure 2). The Z-scores outside a range characteristic of native proteins indicate erroneous structures. Therefore, these results show that our structures modelling are consistent with other proteins in the nature and acceptable for further analysis.

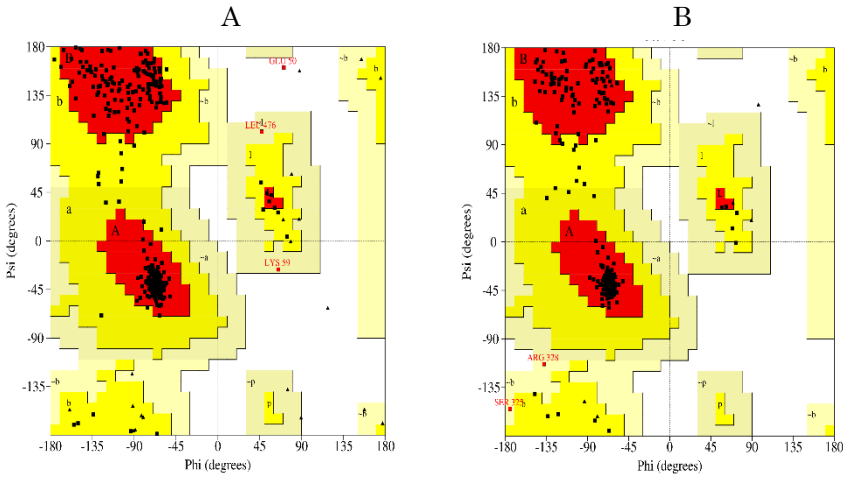

Figure 1. The Ramachandran plot of the best models of GCGR protein for *G. gallus* (**A**) and *G. varius* (**B**). Residues in most favoured regions (**A**, **B**, **L**), Residues in additional allowed regions (a, b, l, p), Residues in generously allowed regions (~a, ~b, ~l, ~p)

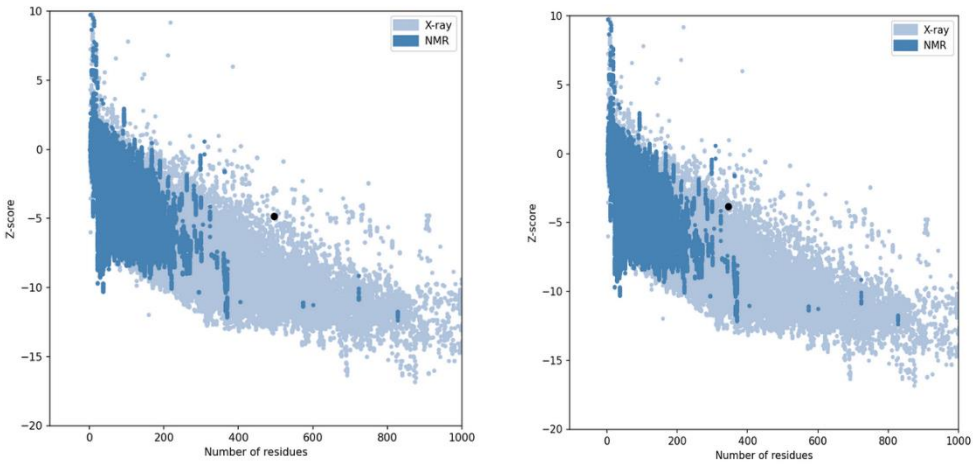

Figure 2. The Z-score of GCGR protein (Black dot) for the best model of *G. gallus* (**A**) and *G. varius* (**B**). The data are based on X-Ray (dark grey) or NMR (light grey) analysis of the proteins in the nature.

[Downloaded from ijls.yu.ac.ir on 2025-10-16]

[DOI: 10.61186/ijls.1.1.33]

Then the best models of GCGR proteins were used for a 50 ns MD simulation at 310 K. The root mean square deviations (**RMSD**) of the protein backbones were calculated during the simulation and are shown in Figure 3. This parameter shows the amount of movement for all the protein atoms compared to their starting structure during MD simulation time. The trivial standard deviation of parameters in Table 2 confirms structural equilibration during the last 10 ns of MD simulation. The more numbers of hydrogen bonds between protein-protein and protein-solvent, and accessible surface area for the GCGR protein of *G. gallus* relative to *G. varius* protein was due to the larger structure of GCGR protein of *G. gallus* or its extra intracellular part.

Table 2. The average RMSD and RMSF of all residues, the average number of hydrogen bonds and solvent accessible surface area during the last 10 ns of MD simulation.

GCGR protein	RMSD (nm)	RMSF (nm)	hbond-pro-pro	hbond-pro-sol	SASA (nm^2)
G. gallus	1.10±0.03	0.14	373.70±11.40	689.67±20.94	237.43±3.91
G. varius	0.88±0.04	0.14	244.42±7.78	484.24±16.45	170.58±2.95

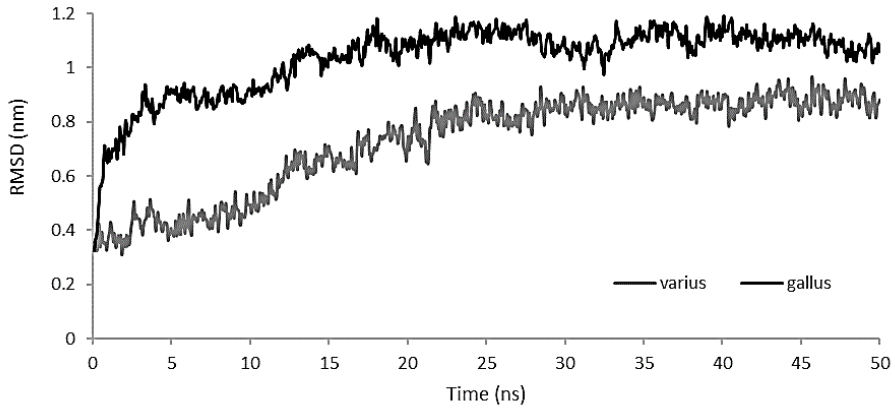

Figure 3. The RMSD of GCGR proteins for *G. gallus* and *G. varius* during 50 ns MD simulation.

.

The results of the RMSD plot show that the backbone of both proteins reached structural equilibrium at 40 ns, and the position of all protein atoms has not changed much in comparison with the starting structures. Therefore, all analyses were done during the last 10 ns. The average temperature during the last 10 ns was 310 K for both GCGR proteins. Table 2 shows the average RMSD and root mean square fluctuation (**RMSF**) of all residues, the average number of hydrogen bonds between protein-protein and protein-solvent, and, the accessible surface area of GCGR proteins during the last 10 ns of MD simulation.

Figure 4 shows the root mean square of the residual fluctuations (**RMSF**) of residues for the two species during the last 10 ns of the simulation.

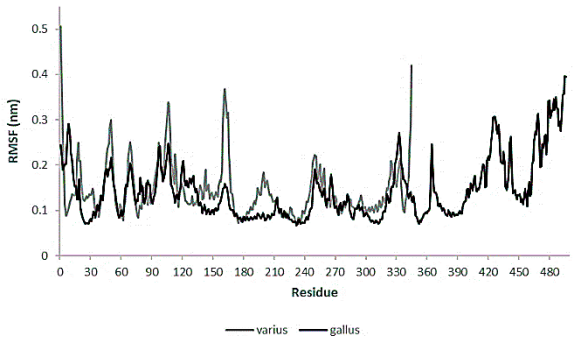

Figure 4. The backbone RMSF for residues of the GCGR protein in *G. gallus* and *G. varius* during the last 10 ns of molecular dynamics simulations.

[Downloaded from ijls.yu.ac.ir on 2025-10-16]

[DOI: 10.61186/ijls.1.1.33]

In the RMSF plot, loop regions, and both C and N terminals show high values, and helix, and beta-sheet structures show low values. The residues 1-22 in both proteins are in the N-terminal and have no structure. The RMSF plot shows that even though the overall flexibility or average RMSF for all residues (Figure 4) in the two species was the same (0.14 nm), deletion of the intracellular part, or residues 346-496, in the GCGR protein of *G. varius* led to an increase in the flexibility of residues in the Gln 22-Tyr 34, Gly 107, Ser 162, and Leu 187-Leu 210 regions. The residues 187-210 have a helix structure, except in the 199-202 region. The increase in flexibility of Arg 345 of the GCGR protein of *G. varius* is because of its location at the C-terminal end of the protein and therefore its free vibration.

Also, the percentage of secondary structures of both GCGR proteins for the extracellular domain, stalk, and intracellular domain during the last 10 ns of MD simulation was calculated (Table 3).

Table 3. The percentage of secondary structure elements in both GCGR proteins during the last 10 ns MD simulation

	Structure	Coil	β-Sheet	Bend	Turn	α-Helix
G. gallus						
Extracellular Domain	0.5	0.31	0.15	0.16	0.19	0.13
Stalk	0.65	0.13	0	0.13	0.17	0.47
Intracellular Domain	0.3	0.39	0.12	0.3	0.11	0
G. varius						
Extracellular Domain	0.51	0.36	0.1	0.12	0.16	0.2
Stalk	0.64	0.21	0	0.11	0.15	0.49

Structure = α-Helix + ß-Sheet + B-Bridge + Turn

The results of Table 3 revealed that the deletion of the intracellular domain in *G. varius* leads to a decrease in several beta-sheet, bend, and turn structures of this protein, while an increase was observed in the number of alpha helix and coil structures in the extracellular domain of GCGR protein in *G. varius*. Also, the coil structure increased in the stalk part of the GCGR in the *G. varius* species. In other words, the omission of the intracellular domain causes a change in the secondary structure of the extracellular domain and stalk parts of the GCGR in the *G. varius* species.

The simulation results also showed that the radius of gyration or tertiary structure and the average number of hydrogen bonds between protein-protein of the stalk of GCGR in the *G. varius* decrease relative to *G. gallus*, and deletion of the intracellular domain causes the shrinking of the GCGR stalk and hydrogen bond reduction. The final structure of the GCGR protein at the end of 50 ns of simulation in *varius* and *gallus* species is shown in Figure 5.

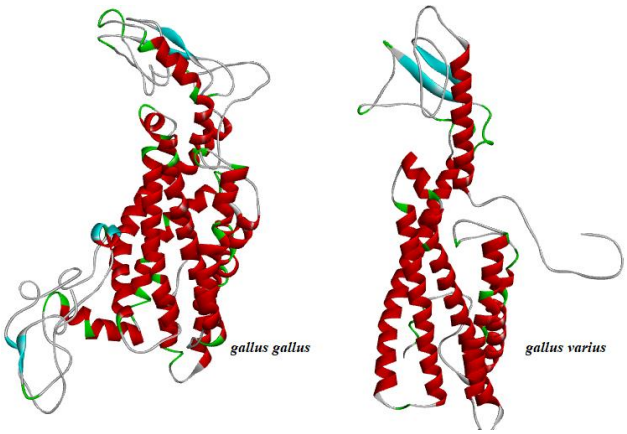

Figure 5. The final structure of GCGR protein at MD simulation in *G. gallus* and *G. varius* species

[Downloaded from ijls.yu.ac.ir on 2025-10-16]

[DOI: 10.61186/ijls.1.1.33]

DISCUSSION

Studies of various living organisms have shown that the control and regulation of blood glucose homeostasis differ among species. Different researches have indicated species-specific differences in blood glucose concentrations among birds, and previous studies have revealed such variations even within the species of the same genus (Braun and Sweazea, 2008). It is mentioned that, the blood glucose level in *G. gallus* is 13.37 mM, while it is 19.95 mM in *G. varius* (Teare, 2013). This suggests that the blood glucose homeostasis in *G. varius* is approximately 1.5 times more than *G. gallus*. To explore the cause of this discrepancy, we compared the genes involved in the blood glucose homeostasis between these two species of the same genus. Studies have shown that glucagon plays a crucial role in maintaining blood glucose concentration; however, unlike mammals, birds are not sensitive to glucose concentration regulation by insulin (Mahnam *et al.*, 2021).

For this reason, we focused on the glucagon precursor gene and their receptors to investigate the difference in blood glucose levels between *G. gallus* and *G. varius*. The glucagon precursor protein is degraded into glistening-related polypeptide (**GRPP**), glucagon, oxyntomodulin (**OXM**), GLP-1, and GLP-2 (Neumiller, 2015). In the glucagon signaling pathway, binding of glucagon to its receptor induces an alteration in receptor conformation, activating the G protein and the adenylate cyclase enzyme. This enzyme produces cyclic adenosine monophosphate (**cAMP**), activating protein kinase A and phosphorylase kinase. Phosphorylase kinase is an enzyme that produces glucose-1-phosphate from glycogen polymers (Tachibana, 2021). We analyzed the genes *GIPR*, *GCGR*, *GLP-2R*, *GLP-1R*, and *GCG* (in the glucagon precursor) in *G. varius* to examine the mutations and their consequences. The mutations identified in *G. varius* are typically not located in different domains or sites of these receptors or hormones. However, several mutations were found that cause amino acid changes and frameshift deletion mutations. Mutations resulting in amino acid changes include GLP1-R, GLP2-R, and GIPR mutations in the signal peptide, the hormone receptor domain, and intermembrane helices 1 and 6, respectively. An important mutation, a frameshift deletion, occurs in the glucagon receptor (**GCGR**) of *G. varius*, leading to a premature termination codon. Consequently, we selected the GCGR gene to investigate its probable effect on the blood glucose differences between the two species, given the significance of the frameshift mutation that results in the deletion of a part of the protein. This mutation causes the deletion from the TM6 region (transmembrane helix 6) in the glucagon receptor to the end of the receptor. TM6 is crucial in the glucagon signaling pathway; when glucagon binds to its receptor, TM6 undergoes a conformational change that facilitates the binding of the G protein to the receptor, initiating signaling (Hilger *et al.*, 2020). We report, for the first time, a mutation that removes TM6—a vital component in the glucagon signaling pathway—from the structure of the glucagon receptor. Interestingly, strains lacking this segment (*G. varius*) exhibit higher blood glucose levels (Teare, 2013; Braun and Sweazea, 2008). We also introduce, for the first time, a species (*G. varius*) that naturally lacks TM6. It has been reported that TM6 creates steric hindrance for the binding of the G protein to the glucagon receptor (Hilger *et al.*, 2020). They concluded that if this hindrance is removed, the G protein is expected to bind more readily to the glucagon receptor, enhancing the signaling pathway and increasing blood glucose levels. This condition is observed in *G. varius*, which lacks TM6 and has elevated blood glucose levels.

CONCLUSION

By modeling and molecular dynamics (**MD**) simulating the GCGR protein in *G. gallus* and *G. varius*, we investigated the proteins based on differences in the number of internal hydrogen bonds, the number of hydrogen bonds with water, the radius of gyration, and the secondary structure. The simulation results also confirmed the structural changes in the glucagon receptor gene in *G. varius*. Therefore, we propose that the c.1021delC

[Downloaded from ijls.yu.ac.ir on 2025-10-16]

[DOI: 10.61186/ijls.1.1.33]

mutation as one of the primary factors contributing to the different stability of the GCGR in *G. varius* versus its phylogenetically close species, *G. gallus*. As a suggestion, the blood glucose variation can be investigated between these two species during different physiological situations such as fasting or feeding, to elucidate the effect of this mutation, in this important blood glucose homeostasis gene, in birds.

ACKNOWLEDGEMENTS

The authors of this paper appreciate Mr. Bani Mehdi`s efforts as expert of genetics laboratory.

CONFLICT OF INTEREST

The authors declare that there is no conflict of interest.

AUTHOR CONTRIBUTIONS

Fatemeh Dashti: Investigation, Writing – original draft preparation. **Karim Mahnam**: Conceptualization, Methodology, Data curation, Writing – review & editing. **Mostafa Shakhsi-Niaei**: Methodology, Data curation, Visualization, Supervision Writing – review & editing.

DATA AVAILABILITY

The datasets generated during and/or analyzed during the current study are presented in the manuscript or are available from the corresponding authors on reasonable request.

ETHICAL CONSIDERATIONS

Not applicable.

FUNDING

This work was partially supported by the Ministry of Science, Research and Technology (Grant No. 141.349).

REFERENCES

Abraham, M.J., Murtola, T., Schulz, R., Páll, S., Smith, J.C., Hess, B., *et al.* (2015) GROMACS: high performance molecular simulations through multi-level parallelism from laptops to supercomputers. Elsevier:19–25.

Braun, E. J., & Sweazea, K. L. (2008) Glucose regulation in birds. Comparative Biochemistry and Physiology Part B: Biochemistry and Molecular Biology, 151(1), 1-9.

Berendsen, H.J.C., van der Spoel, D., van Drunen, R., (1995) GROMACS: A message-passing parallel molecular dynamics implementation. Comput. Phys. Commun. 91, 43–56.

Gundampati RK, Chikati R, Kumari M, Sharma A, Pratyush DD, Jagannadham MV, Kumar CS, Debnath Das M. (2012) Protein-protein docking on molecular models of Aspergillus niger RNase and human actin: a novel target for anticancer therapeutics. J Mol Model. 18(2):653-62. doi: 10.1007/s00894-011-1078-4.

Hilger, D., Kumar, K. K., Hu, H., Pedersen, M. F., O'Brien, E. S., Giehm, L., & Kobilka, B. K. (2020) Structural insights into differences in G protein activation by family A and family B GPCRs. Science, 369(6503), eaba3373.

Idowu, O., & Heading, K. (2018) Hypoglycemia in dogs: Causes, management, and diagnosis. The Canadian Veterinary Journal, 59(6), 642.

Karimi-Shayan, T., Khalaji-Pirbalouti, V., & Shakhsi-Niaei, M. (2017) Evaluation of Glucose Homeostasis in ostrich (Struthio camelus) using Glucose Tolerance Test. Experimental animal Biology, 5(4), 31-38.

Mahnam, K., Shakhsi-Niaei, M., Ziaei, M., & Sweazea, K. L. (2021) In silico evaluation of the downstream effect of mutated glucagon is consistent with higher blood glucose homeostasis in Galliformes and Strigiformes. General and comparative endocrinology, 314, 113925.

Mahnam, K., Foruzandeh, S., Mirakhorli, N., Saffar, B. (2018) Experimental and theoretical studies of cadmium ions absorption by a new reduced recombinant defensin. J. Biomol. Struct. Dyn. 36, 2004–2014. https://doi.org/10.1080/07391102.2017.1340851.

Mahnam, K., Raisi, F., (2017) A theoretical and experimental study of calcium, iron, zinc, cadmium, and sodium ions absorption by aspartame. J. Biol. Phys. 43, 87–103. https://doi.org/10.1007/s10867-016-9435-2.

Mendowski, S., Chapoutot, P., Chesneau, G., Ferlay, A., Enjalbert, F., Cantalapiedra-Hijar, G., & Nozière, P. (2020) Effects of pretreatment with reducing glucoses or an enzymatic cocktail before extrusion of fava bean on nitrogen metabolism and performance of dairy cows. Journal of Dairy Science, 103(1), 396-409.

Neumiller JJ. Incretin-Based Therapies (2015) Medical Clinics of North America. 99(1):107-29.

Norris DO, Carr JA. (2021) Chapter 13 - Comparative aspects of feeding, digestion, and metabolism. In: Vertebrate Endocrinology (Sixth Edition) [Internet]. Sixth Edition. San Diego: Academic Press, 34(1):479-98.

Polakof, S., Panserat, S., Soengas, J. L., & Moon, T. W. (2012) Glucose metabolism in fish: a review. Journal of Comparative Physiology B, 182(8), 1015-1045.

Sali, A., Blundell, T.L., (1993) Comparative protein modeling by satisfaction of spatial restraints. J. Mol. Biol. 234, 779–815.

Sippl MJ. (1995) Knowledge-based potentials for proteins. Curr Opin Struct Biol. 5(2):229-35. doi: 10.1016/0959-440x(95)80081-6.

Tachibana T. (2021) Chapter 26 - Glucagon family. In: Ando H, Ukena K, Nagata S. Handbook of Hormones. 2nd edition. San Diego: Academic Press, 229-30.

Teare, J.A. (ed.): 2013, ISIS Physiological Reference Intervals for Captive Wildlife: A CD-ROM Resource., Species360 , Bloomington, MN.

Van der Spoel, D., Lindahl, E., Hess, B., Groenhof, G., Mark, A.E., Berendsen, H.J.C. (2005) GROMACS: fast, flexible, and free. J. Comput. Chem. 26, 1701–1718. https://doi.org/10.1002/jcc.20291.

Zhang, Y., Qin, C., Yang, L., Lu, R., Zhao, X., & Nie, G. (2018) A comparative genomics study of carbohydrate/glucose metabolic genes: from fish to mammals. BMC genomics, 19(1), 1-14.

[Downloaded from ijls.yu.ac.ir on 2025-10-16]

[DOI: 10.61186/ijls.1.1.33]